JOURNAL OF COMPUTATIONAL PHYSICS 19, 90–109 (1975)

Higher Order Accurate Difference Solutions of Fluid Mechanics Problems by a Compact Differencing Technique

RICHARD S. HIRSH

NASA Langley Research Center, Hampton, Virginia 23665

Received February 11, 1975

A general fourth order differencing scheme proposed by Professor H.-O. Kreiss of Uppsala University is developed and applied to three viscous test problems to verify the accuracy and applicability of the technique. The procedure is atypical since only three nodes are necessary to obtain the desired fourth order accuracy. This is accomplished by a differencing technique which considers the function and all necessary derivatives as unknowns. The relations for these derivatives yield simple tridiagonal equations which can be easily solved. This differencing can be combined with either explicit or implicit time differencing with little difficulty and only a few changes in the solution procedure. The test problems solved are Burgers' equation, Howarth's retarded boundary layer flow, and the incompressible driven cavity. Comparisons of the fourth order results with those computed using second order methods are presented for each test case and clearly indicate that the accuracy achieved by these fourth order computations is always significantly better than current second order procedures.

INTRODUCTION

The ultimate objective of any numerical calculation is the generation of accurate results. As the problems treated become more complex, the standard second order methods become less suitable for use due to the increase in the number of grid points necessary for accuracy. In some cases, the storage requirements of the present-day computers are exceeded. Consequently, higher order methods should be developed and utilized whenever possible.

In a recent report [1] a suggestion made by Kreiss, pertaining to a new compact differencing of fourth-order accuracy, was mentioned. No details of the method were presented and the scheme had not been tested. The present work represents a study of this new method to determine the feasibility of its use as well as to verify the high order of accuracy claimed. No attempt was made during the present study to optimize the computer programs utilized.

The method as originally proposed, and mentioned in reference [1], was conceived to be of use in hyperbolic problems. It was used in that manner by Ciment and Leventhal [2]. However, the present paper will deal with parabolic problems;

either truly time dependent, or marched in some fictitious time to reach an asymptotic steady state. The major difficulty to be overcome using this Kreiss method, as will be noted in the following sections, is the imposition of boundary conditions. Thus, test problems will be presented with increasingly complex boundary conditions.

THE METHOD

The usual objection to fourth order schemes comes from the additional nodes (besides the standard three) necessary to achieve the higher order accuracy. Besides the attendant difficulties of having to consider two fictitious nodes when a boundary point is being computed, the additional nodes almost preclude the use of fourth order implicit methods since the matrix which arises is not the simple tridiagonal form produced by second order schemes. The differencing proposed by Kreiss, however, is fourth order, and compact, that is, it retains tridiagonal form; hence, matrix inversion can be accomplished by the Thomas algorithm.

As suggested by Kreiss, the first and second differences are approximated by

$$y_n' = \left(\frac{D_0}{1 + \frac{1}{6}h^2 D_+ D_-}\right) y_n , \tag{1a}$$

$$y_n'' = \left(\frac{D_+ D_-}{1 + (1/12)\, h^2 D_+ D_-}\right) y_n , \tag{1b}$$

where

$$D_0 y_n = (1/2h)(y_{n+1} - y_{n-1}); \qquad D_+ y_n = (1/h)(y_{n+1} - y_n);$$
$$D_- y_n = (1/h)(y_n - y_{n-1}).$$

In practice, Eqs. (1) are used as follows. Set the derivatives equal to some other function, say

$$y_n' = F_n ; \qquad y_n'' = S_n . \tag{2}$$

Then solve for these new functions F and S from relations obtained after multiplying by the denominator in either (1a) or (1b). These relations are

$$\tfrac{1}{6}F_{n+1} + \tfrac{2}{3}F_n + \tfrac{1}{6}F_{n-1} = (1/2h)(y_{n+1} - y_{n-1}), \tag{3a}$$

$$(1/12)\, S_{n+1} + (5/6)\, S_n + (1/12)\, S_{n-1} = (1/h^2)(y_{n+1} - 2y_n + y_{n-1}). \tag{3b}$$

These two equations yield a tridiagonal matrix for the solution of F or S. With the addition of the defining equation for y, the set of three equations for the three unknowns, y, F, and S, can be solved. The stability properties of this system are discussed in the next section for a linearized model problem.

The accuracy of this scheme is easily obtained by Taylor expansions of Eqs. (3). The resulting truncation error is

$$F_n = y_n' - (1/180)\, h^4 y^{\mathrm{V}}, \tag{4a}$$

$$S_n = y_n'' - (1/240)\, h^4 y^{\mathrm{VI}}. \tag{4b}$$

The usual five-point centered difference scheme of fourth order can also be generated from relations (1). Expanding the denominators by the binomial theorem for small h and keeping only the first terms gives the standard differencing in compact form

$$F_n = D_0(1 - \tfrac{1}{6}h^2 D_+ D_-)\, y_n\,,$$
$$S_n = D_+ D_-(1 - (1/12)\, h^2 D_+ D_-)\, y_n\,.$$

The truncation error here is

$$F_n = y_n' - (1/30)\, h^4 y^{\mathrm{V}}, \tag{5a}$$

$$S_n = y_n'' - (1/90)\, h^4 y^{\mathrm{VI}}. \tag{5b}$$

So, although the new scheme and the standard representation both exhibit fourth order accuracy, the Kreiss scheme should generate slightly more accurate results due to the smaller coefficients of the truncation error terms.

Burgers' Equation

A simple equation which exhibits the interplay of convection and diffusion present in viscous flow problems is Burgers' equation. This equation is generally used as the standard test case for numerical procedures proposed for parabolic equations. The equation is written in a coordinate system moving with the wave so that the steady state waveform can be computed. Thus, the equation to be solved is

$$u_t + (u - \tfrac{1}{2})\, u_x = \nu u_{xx} \tag{6}$$

with $u(-\infty) = 0$ and $u(+\infty) = 1$. The difference form of this equation using Kreiss differencing in space, and simple (first order accurate) forward time differences yields.

$$[(u_i^{n+1} - u_i^n)/\Delta t] + (v - \tfrac{1}{2})\, F_i^m = \nu S_i^m, \tag{7a}$$

$$\tfrac{1}{6}(F_{i+1}^m + 4F_i^m + F_{i-1}^m) = (1/2\Delta x)(u_{i+1}^m - u_{i-1}^m), \tag{7b}$$

$$(1/12)(S_{i+1}^m + 10S_i^m + S_{i-1}^m) = (1/\Delta x^2)(u_{i+1}^m - 2u_i^m + u_{i-1}^m) \tag{7c}$$

where m is either n or $n + 1$.

Note that the time level on the first and second derivatives in Eqs. (7) have not been specified, and the nonlinear convection term has been written as v, as yet, unspecified. The crude time differencing was chosen since the temporal development of the solution is not being sought, only the steady state is required; furthermore, previous experience indicates (and the results verify) that this time truncation error would not be a factor in the final steady state.

Either explicit or implicit methods can be chosen to integrate Eqs. (7), the only difference being the time level chosen for F and S. Choosing the old time level, $m = n$, yields an explicit method. In this case the nonlinear coefficient is simply $v = u_i^n$. An extremely simple integration scheme arises. Given an initial u_i^n, Eqs. (7b) and (7c) immediately yield F_i^n and S_i^n by simple tridiagonal matrix inversions. These derivatives are used in (7a), which yields u_i^{n+1} by quadrature. The simplicity of the method of offset somewhat by stability limitations on the time step. Performing a linear von Neumann stability analysis on Eqs. (7) gives

$$\beta = v\,\Delta t/\Delta x^2 \leqslant \tfrac{1}{3}; \qquad C = v\,\Delta t/\Delta x \leqslant (\tfrac{1}{6})^{1/2} \tag{8}$$

as necessary conditions for stability of the explicit integration. Although these appear to be more restrictive than the usual stability for second order accurate explicit forward time integration [3], i.e.,

$$\beta \leqslant \tfrac{1}{2}; \qquad C \leqslant 1,$$

the actual size of the time step, Δt, can be much larger in the fourth order method if the same accuracy in the solution is desired as is obtainable by second order methods. To obtain similar accuracies, the fourth order method can take significantly larger Δx, and so despite the somewhat smaller β or C, Δt itself is much larger.

Taking the time level of F and S in Eqs. (7) to be $n + 1$ gives a fully implicit system of equations for u, F, and S. The three equations (7) are a coupled set and must be solved simultaneously for the algorithm to be fully implicit. Thus, the integration technique now consists of inverting, at each time step, the block tridiagonal matrix (each block is 3×3) generated by Eqs. (7), instead of the usual scalar tridiagonal matrix. In addition, the nonlinear v must be determined at each time level, either by iteration or extrapolation. Although this entire process is time consuming, it is compensated by the fact that a von Neumann stability analysis shows the implicit integration to be unconditionally stable for all Δt. Similar arguments hold if an implicit Crank–Nicolson integration, where $m = n + \frac{1}{2}$, is chosen.

As the integration of Burgers' equation was the first experiment to be made with the fourth order method, simplicity of the solution procedure was sought. Thus the explicit integration was used. The domain of integration was chosen such that

the region where the wave steepened was well within the solution domain, and therefore *all boundary conditions were assumed known.* The boundary conditions imposed on the numerical solution were $u(+5) = 1$ and $u(-5) = 0$. A linear initial profile was chosen for u, and then the solution was marched in time until the time derivative was found to be some specified small value, and this was assumed to be the converged solution.

Various solutions of Eq. (6) were obtained over a range of ν, Δx, and Δt. Some of these are shown in Table I compared with the exact solution for the steady state, and a second order accurate solution of Burgers' equation for two different grid sizes.

Note that for the larger value of the viscosity ($\nu = \frac{1}{8}$) the fourth order solution is accurate to four decimal places when compared with the exact analytical solution. The second order finite difference scheme, although accurate to two decimal places,

TABLE I

Comparison of Computed Values of Solutions of Burgers' Equation with Exact Analytic Results

	$\nu = \frac{1}{8}$			
x	Exact	Kreiss ($h = 0.2$)	F.D. ($h = 0.2$)	F.D. ($h = 0.05$)
0	0.5	0.50000	0.5000	0.50000
0.2	0.68997	0.69033	0.6999	0.69054
0.4	0.83202	0.83224	0.8447	0.83276
0.6	0.91683	0.91687	0.9269	0.91744
0.8	0.96083	0.96082	0.9673	0.96123
1.0	0.98201	0.98199	0.9857	0.98225
1.2	0.99184	0.99182	0.9938	0.99197
1.4	0.99632	0.99631	0.9973	0.99638
1.6	0.99834	0.99834	0.9988	0.99838
1.8	0.99925	0.99925	0.9995	0.99927
	$\nu = 1/16$			
				Kreiss ($h = 0.1$)
0	0.5	0.50000	0.5000	0.50000
0.2	0.83202	0.83825	0.9000	0.83224
0.4	0.96083	0.95933	0.9878	0.96082
0.6	0.99184	0.99216	0.9986	0.99182
0.8	0.99834	0.99809	0.9998	0.99834
1.0	0.99966	0.99974	1.0000	0.99966
1.2	0.99993	0.99989	1.0000	0.99993

suffers greatly from a lack of accuracy when compared to the fourth order method. A fourfold decrease in the grid size in the second order accurate solution for $\nu = \frac{1}{8}$ still does not give as accurate results as Kreiss' method.

Decreasing the viscosity to $\nu = 1/16$ gives a more striking comparison of relative accuracy, as can be seen in Table I. The Kreiss method still retains fairly good accuracy, wheras the accuracy of the finite difference scheme has deteriorated badly. Burgers' equation has a Reynolds number scaling which gives equal values of u for constant $\nu/\Delta x$. This was tested for the $\nu = 1/16$ case by halving the grid size. Both the Kreiss method, shown in Table I, and the finite difference method reproduced the equivalent $\nu = \frac{1}{8}$, $\Delta x = 0.2$ results when run on a $\Delta x = 0.1$ grid.

The existence of the analytic solution also aids in the estimation of the accuracy of the method since the numerical solution can be compared with it rather than with other numerically computed results. Figure 1 shows the maximum difference

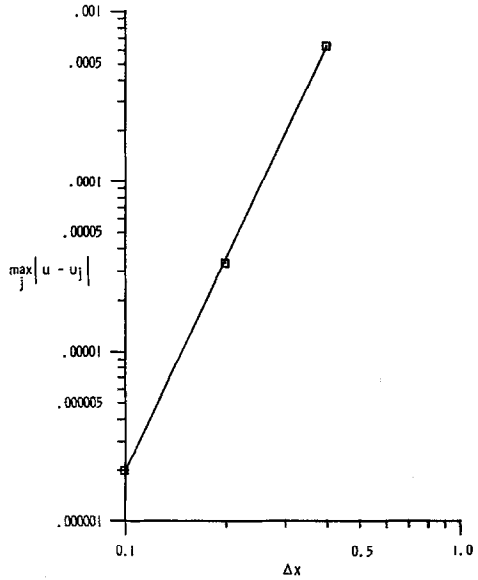

FIG. 1. Convergence rate of Kreiss' method for Burgers' equation.

between the computed solution and the exact analytical solution for three different grid spacings. The slope of the curve gives the exponent in the truncation error which in this case is four. Hence the method converges with fourth order spatial accuracy confirming the estimated truncation error of Eqs. (4).

Note that relation (8) gives an estimate of the work necessary to reach the above steady state solutions for various grid sizes. For Kreiss' method, halving the grid

size means about four times as many steps, since $\Delta t \propto \Delta x^2$. To acheive the same spatial accuracy by a standard second order method, the grid size must be reduced by four. However, the stability restrictions for these explicit methods are essentially the same as those of the fourth order methods, hence the work needed is increased sixteenfold. The validity of the stability restriction (8) was tested by increasing the time step, Δt, for a fixed grid size. Convergence was obtained for $\beta = 0.325$, but for $\beta = 0.350$ (i.e., $\beta > \frac{1}{3}$) the solution diverged confirming the linear von Neumann analysis.

Boundary Layer Equations

The next class of problem examined with Kreiss' method are problems where one boundary condition, necessary for specification of u, F, or S, is unknown. An excellent example of a problem of this type is a nonsimilar boundary layer flow. The incompressible boundary layer equations consisting of the momentum and continutity equations are [4]

$$uu_x + \bar{v}u_y = u_e u_{ex} + \nu u_{yy},$$
$$u_x + \bar{v}_y = 0.$$

These can be written in similarity form by introducing the transformation

$$\xi = x; \qquad \eta = y/(2\nu x)^{1/2}; \qquad \bar{v} = (\nu/2\xi)^{1/2} v$$

which yields

$$2\xi u u_\xi + (v - \eta u) u_\eta = 2\xi u_e u_{e\xi} + u_{\eta\eta}, \tag{9a}$$
$$2\xi u_\xi - \eta u_\eta + v_\eta = 0. \tag{9b}$$

In difference form these become

$$2\xi^{i+1/2} u_j^{i+1/2} \left(\frac{u_j^{i+1} - u_j^{i}}{\Delta\xi}\right) + (v_{j+1/2}^{i+1/2} - \eta_{j+1/2} u_j^{i+1/2}) F_j^{i+1/2}$$
$$= 2(\xi u_e u_{e\xi})^{i+1/2} + S_j^{i+1/2}, \tag{10a}$$
$$\tfrac{1}{6}F_{j+1}^{i+1} + \tfrac{2}{3}F_j^{i+1} + \tfrac{1}{6}F_{j-1}^{i+1} = (1/2\Delta\eta)(u_{j+1}^{i+1} - u_{j-1}^{i+1}), \tag{10b}$$
$$(1/12)\, S_{j+1}^{i+1} + (5/6)\, S_j^{i+1} + (1/12)\, S_{j-1}^{i+1} = (1/\Delta\eta^2)(u_{j+1}^{i+1} - 2u_j^{i+1} + u_{j-1}^{i+1}), \tag{10c}$$

where, for any of the dependent variables

$$g_j^{i+1/2} = \tfrac{1}{2}(g_j^{i+1} + g_j^{i}),$$

where an implicit Crank–Nicolson scheme has been written to integrate the momentum equation; the continuity equation will be discussed shortly. The implicit method was chosen for this problem in order to eliminate the stability difficulties encountered when u approaches the no-slip boundary condition at the wall. Second order integration was chosen since, for this problem, accuracy in the marching direction will be important to trace the history of the boundary layers. The discrepancy between the second order ξ truncation and the fourth order η truncation in Eqs. (10) above lowers the accuracy from fourth order, but better than second order accuracy was expected. To complete the specification of the problem, boundary conditions for all the variables are

$$\eta = 0: \quad u = 0, \qquad v = 0, \qquad S = -2\xi u_e u_{e\xi};$$
$$\eta \to \infty: u = u_e, \qquad F = 0, \qquad S = 0.$$

The boundary condition on S at $\eta = 0$ is obtained by applying the boundary layer equation, (10a), at the wall. The outer edge values on F and S assume that the conditions are applied in the inviscid outer flow. These are all the conditions that can justifiably apply since F at $\eta = 0$ is the shear at the wall, and this is usually what we are seeking to determine. However, for the differencing (10b), the function F is obtained from a tridiagonal matrix, and two boundary conditions are required for the numerical solution.

At each ξ step, the solution procedure consisted of solving the 3×3 block tridiagonal system for u, F, and S generated by Eq. (10), and then solving the continuity equation, (9b), for v. This value of v was then used to generate new values of u, F, and S, and the iteration cycle repeated until convergent values of the first derivative at the wall, the shear, were obtained.

Since the boundary layer equations are iterated at each step, the simplest condition for F which yields fourth order accuracy, and does not destroy the tridiagonal nature of the solution is chosen. A one-sided difference on u is written using the last iterated value, so the boundary condition lags one iterate behind the solution. The form used was

$$F_1 = (-12u_1 + 48u_2 - 36u_3 + 16u_4 - 3u_5)/12\,\Delta\eta. \tag{11}$$

Finally, the integration of the continuity equation must be considered. As mentioned above, continuity was solved for v after the momentum equation was solved for u, F, and S. The integration of the continuity equation was accomplished by the standard second order scheme

$$v_j^{i+1/2} = v_{j-1}^{i+1/2} - \Delta\eta[\xi^{i+1/2}(u_{\xi_j}^{i+1/2} + u_{\xi_{j-1}}^{i+1/2}) - \eta_j F_{j-1/2}^{i+1/2}] \tag{12a}$$

or by a fourth order scheme

$$v_j^{i+1/2} = v_{j-1}^{i+1/2} - \tfrac{1}{6}\Delta\eta[2\xi^{i+1/2}(u_{\xi_j}^{i+1/2} + 4u_{\xi_{j-1/2}}^{i+1/2} + u_{\xi_{j-1}}^{i+1/2}) - (\eta_j F_j^{i+1/2} + 4\eta_{j-1/2}F_{j-1/2}^{i+1/2} + \eta_{j-1}F_{j-1}^{i+1/2})], \tag{12b}$$

where the half-point values $(j - \frac{1}{2})$, are obtained from fourth order Lagrangian interpolation. Both schemes were used in the calculations to be shown.

As a test problem for the boundary layer equations, the classical linearly retarded boundary layer past a flat plate, originally solved by Howarth [5], was used. Using the notation of the present paper we have

$$u_e = 1 - \xi.$$

In addition to Howarth's local similarity series solution, this problem has been treated numerically by Smith and Clutter [6], and Keller and Cebeci [7], among others, affording the problem a convenient check of numerical solutions.

The aim in the Howarth problem is an accurate prediction of ξ history of the flow, so the $\xi = 0$ initial solution needs to be predicted accurately. If ξ is set equal to zero in Eqs. (10), the classical Blasius similarity boundary layer equations are obtained [4]. The Kreiss differencing procedure was used to generate a Blasius profile to start the Howarth solution. Since this profile is obtained by marching Eq. (10) to similarity (ξ derivatives equal zero), again, as in the steady Burgers' solution, the results should be close to fourth order, due to the elimination of the second order ξ truncation error.

Figure 2 gives the Blasius profile for five different values of $\Delta\eta$. The symbols are shown only for the largest value $\Delta\eta = 1.0$. On the scale used for this plot, no difference can be distinguished between any of the calculations.

Table II compares the first derivative of u at the wall computed by the Kreiss method, with those of one of the best second order schemes available, the Keller–Cebeci box method [7]. Note that for any comparable $\Delta\eta$ the fourth order method gives significantly better accuracy than the box method when compared with the exact value of $F_w = 0.469600$. Even for the crude $\Delta\eta = 0.2$ mesh, the Kreiss scheme generates fourth decimal place accuracy. These results were obtained using the fourth order Runge–Kutta continuity solver. When the second order continuity scheme was used, only fifth decimal place changes were apparent.

The results used the implicit, block tridiagonal inversion scheme mentioned in the Burgers' equation section of this paper. Step sizes four orders of magnitude greater than the diffusive stability limit were used with no adverse effect on the stability properties. The lagged boundary condition on F appeared to have no affect on the procedure.

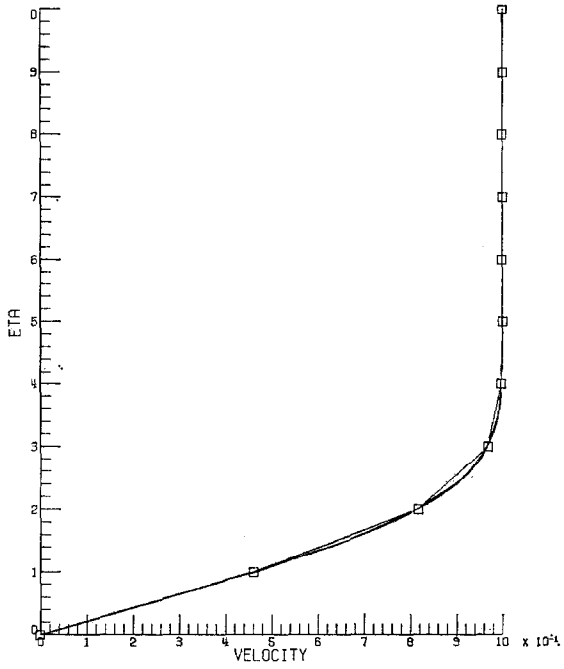

FIG. 2. Calculated Blasius profile for five values of $\Delta\eta$.

TABLE II

Fourth Order and Second Order Computations of Blasius Shear Function at the Wall

$\Delta\eta$	Kreiss	Box
1.0	0.430834	0.506065
0.5	0.465713	0.478914
0.4	0.468430	
0.333		0.473753
0.3	0.469381	
0.2	0.469582	
0.1	0.469599	0.469975
0.05		0.469694
0[a]		0.469601

[a] The most accurate value obtained (using Richardson extrapolation).

With the computed Blasius solution as an initial value, the Howarth problem was computed for various grid sizes. In the initial region of the flow where Howarth's series is accurate, again the Kreiss scheme for a $\Delta\eta = 0.2$ gave four decimal place accuracy compared to Howarth. However, in this type of flow, the point of separation is of utmost significance. Some numerical procedures have difficulty approaching separation; this was not encountered with the Kreiss method. Table III shows the calculated separation point for various values of $\Delta\eta$. Other calculated values found in the literature are $\xi_{sep} = 0.119813$ quoted by Rosenhead [4]; $\xi_{sep} = 0.11985$ calculated by Keller and Cebeci [7] and $\xi_{sep} = 0.120$ estimated by Smith and Clutter [6].

TABLE III

Calculated Position of the Separation Point in Howarth Flow

$\Delta\eta$	ξ_{sep}
0.5	0.119989
0.4	0.119893
0.3	0.119839
0.2	0.119818

All the fourth order values given in Table III were computed using the fourth order continuity integration. When the second order integration was used no difficulty ensued in the ξ integration nearing separation, but ξ_{sep} exceeded 0.120 for all $\Delta\eta$ values used. Thus, the small change in the wall derivative noted in the Blasius solution becomes important when the point of separation, defined as that ξ where $F_w = 0$, is approached.

Incompressible Driven Cavity

As the final test of the Kreiss differencing procedure, an extension to two spatial dimensions was chosen. The incompressible driven cavity was originally solved analytically [8], and followed by a numerical solution using relaxation techniques [9]. Recently, it has again become the study of some numerical experiments [10, 11, and unpublished results obtained at NASA Langley]. This flow is an excellent test case since it exhibits extreme boundary complications in addition to the added spatial dimension.

The geometry consists of a square cavity filled with an incompressible fluid. At the initial time the upper wall is given a unit velocity (see Fig. 3), and the final,

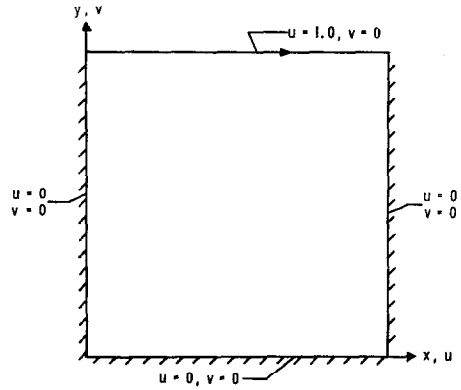

FIG. 3. Schematic of incompressible driven cavity showing geometry, and velocity boundary conditions.

asymptotic, steady state solution is sought. The equations of incompressible flow, in terms of the vorticity and stream function, cast in nondimensional form are

$$\zeta_t + u\zeta_x + v\zeta_y = (1/R)(\zeta_{xx} + \zeta_{yy}), \tag{13}$$

$$\nabla^2\Psi = \zeta. \tag{14}$$

where

$$u = \Psi_y, \qquad v = -\Psi_x$$

The boundary conditions which can be specified are, on all four bounding sides,

$$\Psi = \text{const} = 0; \tag{15a}$$

$$\Psi_x = -v, \qquad \Psi_y = u; \tag{15b}$$

and

$$\nabla^2\Psi = \Psi_{xx} = \zeta; \qquad x = 0 \& x = 1; \tag{16a}$$

$$\nabla^2\Psi = \Psi_{yy} = \zeta; \qquad y = 0 \& y = 1. \tag{16b}$$

No other physical conditions exist.

The implicit integration formulation of the Kreiss procedure is desired, since the explicit stability restriction (through the cell Reynolds number) prevents the calculation of any significant Reynolds number flow; a test case of $R = 100$ was desired. To retain the tridiagonal nature of the matrices involved, an ADI type time marching procedure was formulated. Thus, to take one full time step in the vorticity transport equation requires the solution of

$$\frac{1}{\Delta t}(Z^*_{i,j} - Z^n_{i,j}) + u \cdot ZFX^n_{i,j} + v \cdot ZFY^*_{i,j} = \frac{1}{R}(ZSX^n_{i,j} + ZSY^*_{i,j}), \tag{17a}$$

$$\frac{1}{\Delta t}(Z^{n+1}_{i,j} - Z^*_{i,j}) + u \cdot ZFX^{n+1}_{i,j} + v \cdot ZFY^*_{i,j} = \frac{1}{R}(ZSX^{n+1}_{i,j} + ZSY^*_{i,j}), \tag{17b}$$

where

$$Z = \zeta, \qquad ZFX = \zeta_x, \qquad ZSX = \zeta_{xx},$$

etc. To complete the formulation, Kreiss relations similar to Eqs. (3) have to be included for evaluation of ZFY^*, ZSY^*, ZFX^{n+1}, ZSX^{n+1}. At each half-step of the ADI procedure, a block tridiagonal matrix is inverted for ζ and its two derivatives.

After completion of the complete ADI step, the Poisson equation is cast in a time dependent form

$$\nabla^2 \Psi = \zeta + \Psi_\tau \tag{18}$$

and solved by the ADI extension of the Kreiss procedure. Since the asymptotic steady solution is sought, the Poisson equation (18) is not solved to convergence at each corresponding ζ time step. Rather, the solution Ψ is simply made consistent with the new ζ values by taking a reasonably small number (five were used for all the following) of fictitious time steps $\Delta\tau$.

Central to the use of this fourth order procedure is the requirement that boundary conditions be specified for the derivatives of the function being solved for, in addition to the function itself. For the solution of Ψ, Eqs. (15) and (16) give all the necessary information needed on the boundaries, assuming ζ is known from the previous time step. But, this ζ calculation also needs boundary conditions, and none exist physically. The vorticity equation, (13), can be written on the boundary at each ADI step to provide a relation for the second derivatives. However, no simple evaluation of ζ or its first derivatives is apparent. This was noted in a previous attempt to solve this problem [12]. Thus, here is a case where two boundary conditions are unknown. Actually, as will be shown later, there are even more.

The solution to this difficulty can be accomplished by the following argument. The simple question can be asked: What is the most accurate relation which can be written relating any function and its first two derivatives by a one-sided differencing, and still retain a tridiagonal form? That is, what is the best accuracy attainable by

$$Ag_i + Bg_{i+1} + CF_i + DF_{i+1} + ES_i + GS_{i+1} = 0,$$

where $F = g'$, $S = g''$ and A to G are constants to be determined? The result is a relation containing one free parameter, K:

$$g_i - g_{i+1} + h[KF_i + (1 - K) F_{i+1}] + \frac{h^2}{2}[(K - \tfrac{1}{3}) S_i + (K - \tfrac{2}{3}) S_{i+1}] + \frac{h^4}{12}(K - \tfrac{1}{2}) g^{IV} = 0. \tag{19}$$

Note the order of the truncation error.

There are some very obvious choices for K. First choose $K = 1$ or $K = 0$. These give the relations

$$g_i - g_{i+1} + hF_i + h^2(\tfrac{1}{3}S_i + \tfrac{1}{6}S_{i+1}) + O(h^4) = 0, \tag{20a}$$

$$g_i - g_{i+1} + hF_{i+1} - h^2(\tfrac{1}{6}S_i + \tfrac{1}{3}S_{i+1}) + O(h^4) = 0, \tag{20b}$$

which isolate the first derivative at a point. Equations (20) are identical to the spline relations given by Rubin and Graves [11]. Another simple choice, $K = \frac{1}{3}$ or $K = \frac{2}{3}$ isolates the second derivative at a point.

$$g_i - g_{i+1} + h(\tfrac{1}{3}F_i + \tfrac{2}{3}F_{i+1}) - (h^2/6)\,S_{i+1} + O(h^4) = 0, \tag{21a}$$

$$g_i - g_{i+1} + h(\tfrac{2}{3}F_i + \tfrac{1}{3}F_{i+1}) + (h^2/6)\,S_i + O(h^4) = 0. \tag{21b}$$

The final choice for the parameter is $K = \frac{1}{2}$. This eliminates the fourth order truncation error, yielding an expression of higher order,

$$g_i - g_{i+1} + (h/2)(F_i + F_{i+1}) + (h^2/12)(S_i - S_{i+1}) + O(h^5) = 0. \tag{22}$$

This relation has been given before by Liniger and Willoughby [13], in a somewhat different form, and is called by them the second diagonal Padé approximant.

Any of these relations (20)–(22) can be used to generate the additional boundary conditions necessary for ζ and its first derivatives. Using the Padé approximation (22), for example, written in terms of Ψ, and its derivatives normal to the boundary $y = 1$ gives

$$\Psi_{i,j} - \Psi_{i,j+1} + (h/2)(\Psi FY_{i,j} + \Psi FY_{i,j+1}) + (h^2/12)(\Psi SY_{i,j} - \Psi SY_{i,j+1}) = 0.$$

But, from, (16), we know the relation between ζ and the second derivatives, thus at the upper wall

$$\zeta_{i,j+1} = \Psi SY_{i,j} + (12/h^2)\,\Psi_{i,j} + (6/h)(1 + \Psi FY_{i,j}). \tag{23}$$

Here note the truncation is $O(h^3)$ since the relation (23) is written for the second derivative of Ψ and not Ψ itself. Using the Padé approximant written in terms of ζ gives the desired relation for the first derivative at a wall.

The same methodology holds when the lower order relations are to be used. Since the first and second derivatives appear very simply in (20) and (21), Eqs. (20) are used to generate the first derivatives of ζ at the boundaries, and ζ at the boundaries is obtained from equation (20) written for Ψ.

The suitability of the higher order conditions (22), has been tested by a boundary stability analysis. For a simple scalar parabolic equation, boundary conditions given by Eq. (22) can be shown to satisfy the requirements given by Varah [14] for parabolic equations.

Two other details of the integration scheme need elaboration. It was mentioned that the second derivative of ζ could be calculated from the governing equation, (13). This is true on any of the bounding surfaces where the velocity vanishes exactly, for then, no first derivatives appear. But on the driven wall, $u = 1$, and the equation is

$$\zeta_t + \zeta_x = (1/R)(\zeta_{xx} + \zeta_{yy})$$

Thus a coupling between unknown boundary values of ζ_{xx} and ζ_x occurs, and a consistent fourth order evaluation of ζ_x using the compact relation for the first derivative, Eq. (3a), must be included in Eq. (24).

The other boundary condition difficulty that arises is the correct prescription of ζ^*, the zeta value at the first ADI step. The usual ADI scheme is second order in time, but Fairweather and Mitchell [15] have shown that this can be degraded by rapidly time varying ζ, and give the correct conditions to apply to retain the second order accuracy. Since only the steady state solution to this cavity problem is sought it was hoped that the application of $\zeta_{i,j}^{n+1}$ at the first step would suffice. This would not work, and so

$$\zeta_{i,j}^* = \tfrac{1}{2}(\zeta_{i,j}^n + \zeta_{i,j}^{n+1})$$

was used successfully instead of the true second order accurate condition. No attempt was made to incorporate Fairweather's conditions because the actual time accuracy was unimportant here.

RESULTS

The cavity problem was run for a standard test case of $R = 100$ on a 15×15 grid with a time step equal to the CFL limit. Both Padé boundary conditions (22), and the lower order spline boundary conditions (20), (21) were used in the calculations. A plot of stream function and vorticity contours are shown in Figs. 4 and 5. The numerical results were compared with the spline calculations of Rubin and Graves [11] on the same grid, and some second order finite difference solutions obtained at NASA Langley using the ADI method on the same grid, and on a finer 57×57 grid. The 15×15 ADI calculations agree exactly with the published values of Mills [9].

The fine grid second order solutions were very well approximated by the Kreiss procedure on the standard 15×15 brid. Table IV shows the value of the vorticity on the upper wall. Note the excellent agreement of the fourth order method with the very accurate second order solution. This agreement is even better for the-stream function values in the row through the maximum Ψ point. This is shown in Table V.

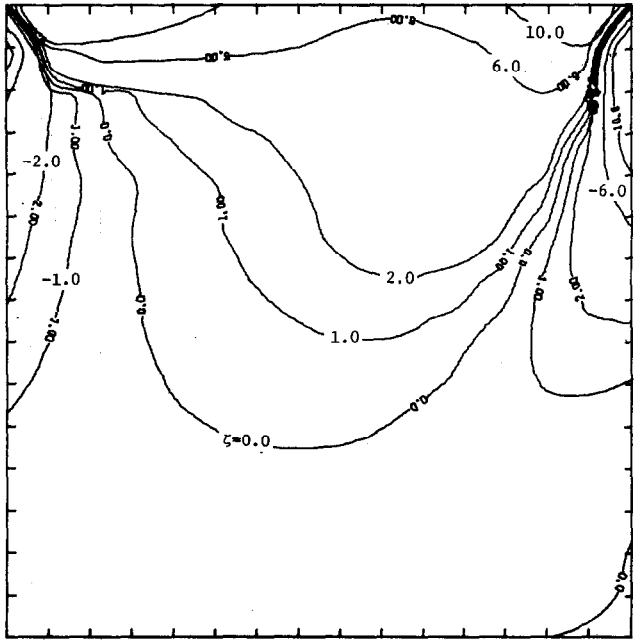

FIG. 4. Vorticity contours for $R = 100$ driven cavity.

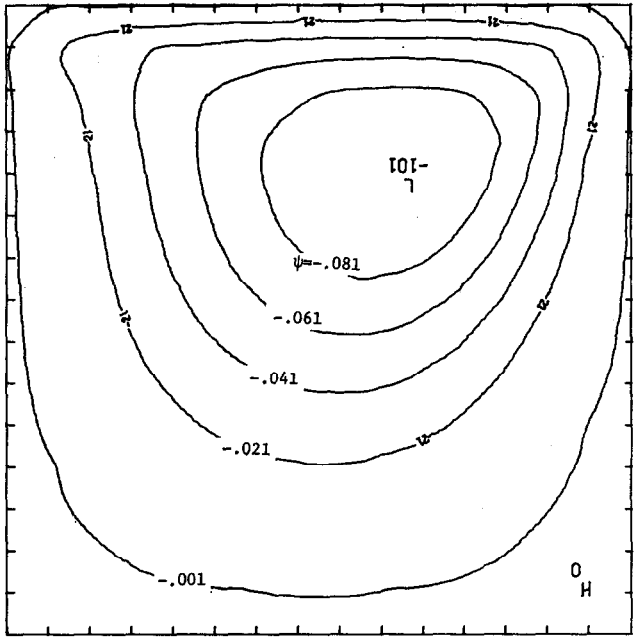

FIG. 5. Stream function contours for $R = 100$ driven cavity.

TABLE IV

Calculated Values of the Vorticity at the Moving (Upper) Wall for Various Methods

	X												
Method	0.0714	0.1428	0.2143	0.2857	0.3571	0.4286	0.5000	0.5714	0.6428	0.7143	0.7857	0.8571	0.9286
A	38.05	20.99	14.95	11.59	9.338	7.749	6.696	6.187	6.317	7.254	9.314	13.45	25.37
B	34.80	21.00	15.05	11.78	9.591	8.033	6.927	6.380	6.293	7.226	8.968	14.23	27.63
C	35.36	23.83	17.18	13.12	10.42	8.568	7.237	6.613	6.307	7.281	8.414	13.41	23.70
D	32.92	21.28	15.88	12.49	10.15	8.374	7.137	6.390	6.192	6.673	8.026	11.14	24.19
E	24.04	20.04	16.74	14.10	11.97	10.26	8.916	7.948	7.423	7.477	8.329	10.44	14.86

Note. A, second order ADI on 57 × 57 grid; B, Kreiss method with high order boundary conditions (Eq. (22)) on 15 × 15 grid; C, Kreiss method with low order boundary conditions (Eqs. (20), (21)) on 15 × 15 grid; D, cubic spline method of Ref. [12]; E, second order ADI on 15 × 15 grid.

581/19/1-8

TABLE V

Calculated Values of the Stream Function on the Row Containing the Maximum Stream Function ($y = 0.7143$) for Various Methods[a]

	X												
Method	0.0714	0.1428	0.2143	0.2857	0.3571	0.4286	0.5000	0.5714	0.6428	0.7143	0.7857	0.8571	0.9286
A	−0.0064	−0.0209	−0.0381	−0.0555	−0.0710	−0.0844	−0.0948	−0.1009	−0.1013	−0.0940	−0.0768	−0.0488	−0.0163
B	−0.0065	−0.0212	−0.0385	−0.0556	−0.0713	−0.0846	−0.0949	−0.1010	−0.1014	−0.0944	−0.0775	−0.0497	−0.0173
C	−0.0063	−0.0206	−0.0377	−0.0547	−0.0703	−0.0837	−0.0940	−0.1000	−0.1004	−0.0931	−0.0759	−0.0480	−0.0162
D	−0.0064	−0.0211	−0.0390	−0.0570	−0.0735	−0.0875	−0.0983	−0.1047	−0.1053	−0.0980	−0.0802	−0.0509	−0.0173
E	−0.0053	−0.0162	−0.0293	−0.0427	−0.0557	−0.0673	−0.0769	−0.0835	−0.0856	−0.0813	−0.0686	−0.0462	−0.0180

[a] See Table IV for legend.

Note. Method E actually predicts $\Psi_{max} = -0.0874$ at $x = 0.6428$, but $y = 0.7857$.

All boundary values for Ψ and its derivatives are known, so any inconsistencies introduced by either relations (20), (21), or (22) are avoided, and Ψ values more accurate than the ζ values are produced.

Other characteristics of the 57 $\times$ 57 calculations were also reproduced. The u-velocity in the upper left corner was calculated to be negative for the fine grid and also by the Kreiss scheme. The very small pocket of recirculating flow evidenced by a positive Ψ in the lower right-hand corner of Fig. 5 did not appear in the 15 $\times$ 15 second order calculation but was calculated in the 57 $\times$ 57 case.

TABLE VI

Calculated Value of the Velocity, u, at the Point (0.9286, 0.0714)[a]

Method	u_{corner}
A	−0.0662
B	−0.1184
C	−0.1327
D	−0.1323
E	+0.0573

[a] See Table IV for legend.

Without presenting the full output for each of the methods, further comparisons are difficult, but in summary the Kreiss method showed extreme accuracy when compared to second order methods on the same grid. Needless to say the equivalent comparison of the Kreiss scheme on the 15 $\times$ 15 grid and the second order scheme on the 57 $\times$ 57 grid showed a saving of a factor of 20 in computer run time and a storage saving of about 3.

One final test was performed to test the stability characteristics of the implicit method used. The time step was raised to five times the CFL limit and the same steady state solution was generated in one-third the computing time. A rise to ten times the CFL limit caused the solution to diverge, but this is not surprising since the coefficients u and v in Eq. (13) are computed at the old time level, n, and only a few steps are taken in the Poisson solver. Thus, the linearization scheme deprives the technique of its true unconditional stability.

CONCLUSIONS

The compact fourth order differencing method proposed by Kreiss has been shown to be an effective technique in the computation of fluid mechanics problems. The accuracy of the method is unquestionably higher than second order methods,

and where exact solutions exist, has been shown to be fourth order. The method is stable under a variety of applied boundary conditions of varying order. A high order Padé boundary condition (22) has been shown to be the best condition which can be used given the restriction of a tridiagonal form, and this condition gives the most accurate results when used in conjunction with Kreiss' differencing technique. Thus, Kreiss' method should be of great value in problems where storage limitations preclude second order methods, or even for general problems since the coding is simple, and time and storage requirements are quite low.

REFERENCES

1. S. A. ORSZAG AND M. ISRAELI, Numerical Simulation of Viscous Incompressible Flows, Flow Research Report No. 17, Flow Research, Inc., Kent, Wash.; Also see "Annual Reviews of Fluid Mechanics," Vol. 6 (M. Van Dyke, Ed.), Annual Reviews, Inc., Palo Alto, Calif., 1974.
2. M. CIMENT AND S. H. LEVENTHAL, Higher Order Compact Implicit Schemes for Hyperbolic Equations, Paper presented at SIAM 1974 Fall Meeting, October 23–25, 1974, Alexandria, Va.
3. P. J. ROACHE, "Computational Fluid Dynamics," Hermosa Publishers, Albuquerque, N. Mex., 1972.
4. L. ROSENHEAD, "Laminar Boundary Layers," Oxford University Press, London/New York, 1963.
5. L. HOWARTH, *Proc. Roy. Soc. London, Ser. A* **164** (1938), 547–579.
6. A. M. O. SMITH AND D. W. CLUTTER, *AIAA J.* **1** (1963), 2062–2071.
7. H. B. KELLER AND T. CEBECI, in "*Proceedings of the 2nd Intern. Conference on Numerical Methods in Fluid Dynamics*," Springer–Verlag, Berlin, 1971.
8. O. R. BURGGRAF, in "*Proceedings of the* 1965 *Heat Transfer and Fluid Mechanics Institute*," Stanford University Press, Stanford, Calif., 1965.
9. R. D. MILLS, *J. Roy. Aero. Soc.* **69** (1965), 714–718.
10. J. BOZEMAN AND C. DALTON, *J. Computational Phys.* **12** (1973), 348–363.
11. S. G. RUBIN AND R. A. GRAVES, A Cubic Spline Approximation for Problems in Fluid Mechanics, Technical Report 74-T1, Old Dominion University, Norfolk, Va., 1974.
12. R. S. HIRSH, Application of a Fourth Order Differencing Technique to Fluid Mechanics Problems, Paper presented at SIAM 1974 Fall Meeting, October 23–25, 1974, Alexandria, Va.
13. W. LINIGER AND R. A. WILLOUGHBY, *SIAM J. Numer. Anal.* **7** (1970), 47–66.
14. J. M. VARAH, *SIAM J. Numer. Anal.* **8** (1971), 598–615.
15. G. FAIRWEATHER AND A. R. MITCHELL, *SIAM J. Numer. Anal.* **4** (1967), 163–170.